Tuijin Jishu/Journal of Propulsion Technology
ISSN: 1001-4055
Vol. 44 No. 3 (2023)

Simulation of Sandy Soil Shear Characteristics: Calibration and Validation of DEM Contact Models

V.Vinothkumar[1]*, P.Dhananchezhiyan[2], A. Raviraj[3], P. Kamaraj[4], M. Baskar[5]

[1]*Ph.D. Student, Department of farm machinery and power engineering, AEC & RI, TNAU, India*

[2]*Assistant professor, Department of farm machinery and power engineering, AEC & RI, TNAU, India*
[3]*Dean, Agricultural Engineering College and Research Institute, TNAU, India*
[4]*Associate professor, Department of Post Harvest Technology, HC & RI, Periyakulam, TNAU, India*
[5]*Professor, Department of soil science and analytical chemistry, ADAC & RI, TNAU, India*

Abstract: In this study, the behavior of sandy soil has been comprehensively investigated through the application of the Discrete Element Method (DEM) in various moisture and density conditions. Three distinct contact models, including Hertz-Mindlin (HM), Hysteretic Spring (HS), and Hertz-Mindlin with JKR (HM+JKR), have been meticulously evaluated for their performance in replicating the intricate interactions and mechanical responses observed in sandy soil particles under different loading conditions. Laboratory Direct Shear Tests (DSTs) were conducted to obtain empirical data, and the simulation results were subsequently compared with these experimental findings to validate the models. The HM model exhibited notable efficacy in simulating dry soil conditions, while the HS model excelled in capturing the behavior of moist soil, and the HM+JKR model demonstrated superior performance in representing wet soil conditions. The relative errors between simulated and measured yield forces remained within acceptable limits across all models, affirming their reliability in characterizing soil behavior. These calibrated models will prove invaluable in future simulations and analyses of soil-tool interactions in agriculture and geotechnical engineering applications. This research has significantly contributed to a deeper understanding of the Discrete Element Method's capabilities in modeling soil mechanics and has offered valuable insights into the selection of appropriate contact models tailored to distinct soil conditions.

1. Introduction

Before designing machines that handle materials, it is essential to understand the behavior of material shear. In agriculture, engineers and researchers designing tillage and seeding equipment, such as plows, chisels, sweeps, and openers, must be aware of the mechanical properties of soil that these tools interact with during field operations (McKyes,1985). Soil shear properties, typically including soil internal friction and cohesion, are crucial in soil-tool interactions since they impact the tool’s draft force and soil disturbance (Kezdi,1979).

The density and moisture content of soil are among the key factors that impact soil cohesion and friction (Gitau et al.,2008). Two common tests aredirect shear tests (DSTs) and triaxial tests to determine soil internal friction and cohesion. DSTs are typically easier to conduct, but both tests require specialized equipment like a direct shear box or triaxial system, which may not always be available. Additionally, these measurements tend to take more time than a modeling approach. The Discrete Element Method (DEM) is often used to model the mechanical behaviors of soil, such as soil deformation when exposed to a rigid wheel (Khot et al.,2007).Various software applications have been employed for soil modeling utilizing DEM, each offering distinct features and capabilities. The EDEM software is preferred due to its comprehensive simulation and analysis tools (Shi et al., 2019). Its preference can be attributed to its efficient handling of particle-based simulations, accurate representation of soil behavior, and robust visualization options. EDEM has been utilized in numerous studies to model soil mechanics and geotechnical processes (Li et al. (2011),Zhang et al. (2021)). The software's ability to capture granular material interactions, such as particle-particle and particle-surface interactions, provides a detailed representation of soil dynamics and deformation. Moreover, EDEM's advanced post-processing tools enable the extraction of valuable insights from simulated data, aiding in understanding soil behaviors during different loading conditions. This has been demonstrated in studies investigating landslides, soil compaction, and slope stability

(Cundalland Strack(1979),Zhang and Li (2006)).

DEM represents soil material as groups of balls, clusters, or clumps of balls that touch each other. When an external force acts on the material, individual balls shift, causing changes in the dynamics of the material body, including its displacements and forces.

The choice of contact model in simulating soil using the Discrete Element Method (DEM) is paramount as it significantly influences the accuracy and realism of the simulation results. The contact model dictates how forces are transmitted between individual particles in a DEM simulation. Different types of soils exhibit diverse particle interactions, such as cohesive behavior in clayey soils and frictional behavior in granular soils. Hence, selecting an appropriate contact model directly impacts the representation of inter-particle forces, particledeformation, and overall system behavior.

Much literature has highlighted that using an unsuitable or oversimplified contact model can lead to unrealistic simulation outcomes. Simulating granular soils like sand or gravel with a contact model that neglects particle friction might result in an inaccurate representation of shear strength and particle interactions. Research byCundall and Strack(1979) highlighted the necessity of incorporating normal and tangential forces in the contact model to capture particle interactions accurately. Incorporating tangential forces (friction) is especially important in simulating soil with irregular particle shapes and non-cohesive behavior. Studies byPotyondy and Cundall (2004) further emphasized that an appropriate contact model should consider particle size, shape, and surface roughness to achieve accurate simulation outcomes.

When describing particle contacts using a DEM model, calibration of the model parameters is necessary. The micro-properties of balls and bonds are considered as the model parameters in DEM models. To ensure that the model particles represent the soil particles, the behaviors of the model particle must be matched with the behaviors of the simulated soilNitka and Grabowski (2021). This is how the model parameters are usually determined.

Simulation of DST has been carried out using EDEM. Thornton and Zhang(2003), as well asKadau et al. (2006), focused on studying the shear behavior of general granular and interpreting the simulation results. Van der Linde(2007) utilized DST in calibrating model parameters of a DEM model, particularly in simulating soil-tool interaction. Other DEM models simulated DST of non-soil materials, like the aluminum rods tested byLi et al. (2019). Their goal was to enhance the test device to reduce the impact of frictional force on the measured shear strength. The simulation of DST for semi-solid manure was carried out by Landry and team using PFC3D. Their aim was to analyze Micro-properties' influence on the simulation results and compare the simulated internal friction angle and cohesion with the measured values to calibrate the micro-properties. DEM was employed byCoetzee and Els (2009) to simulate shear and compression tests on corn. This was done to calibrate the micro-properties of corn, which could then be used in modeling silo discharge and bucket filling.

The research aims to address the critical question of selecting an appropriate contact model for accurately simulating the behavior of sandy soil through Discrete Element Method (DEM) simulations. The investigation focuses on comparing three distinct contact models: the Hertz-Mindlin contact (HM), Hertz-Mindlin with JKR (HM+JRK) and the Hysteretic Spring (HS) model. This research's primary objective is to assess these contact models' performance in replicating the intricate interactions and mechanical responses exhibited by sandy soil particles under varying loading conditions. Discrete Element Simulations will be conducted using each of the aforementioned contact models. The Dynamic Shear Testing (DST) methodology will be employed as the experimental benchmark for comparison. The DST involves subjecting sandy soil samples to shear loading conditions that mimic those experienced in natural settings. By systematically varying shear rates and normal stresses, the study aims to capture the complex interplay of forces and deformations intrinsic to sandy soil behavior.

2. Methodology

2.1 Laboratory direct shear tests (DST)

Shear properties of sandy soil, such as yield point, cohesion (c), and soil internal friction angle (^), were measured through laboratory DSTs. These tests provided data for developing a model, which is explained in detail later in this paper. The DST apparatus and procedure are described in the following sections.

2.1.1 Test apparatus

An apparatus depicted in Fig:1a was utilized to conduct direct shear tests. The apparatus comprised a soil shear box, a loading head, a weight hanger, and weights to apply normal loads. The soil shear box contained two square rings to secure the soil sample Fig:1b . The box had a cross-section of 60 by 60 mm and a height of 50 mm. A motor was used to achieve horizontal displacement of the shear box, measured with a dial gauge. A proving ring measured the shear force.

Figure 1: Direct shear test apparatus: (a) test setup; (b) shear box

Moisture level	Density level	Misture content	Bulk density *(Mg/m^3)*
Dry	Loose	8.0%	1.40
	Soft	7.5%	1.55
	Firm	7.0%	1.70
	Compact	6.5%	1.85
Moist	Loose	10.0%	1.42
	Soft	9.5 %	1.57
	Firm	9.0 %	1.72
	Compact	8.5%	1.87
Wet	Loose	15.0%	1.44
	Soft	14.5%	1.59
	Firm	14.0%	1.74
	Compact	13.5 %	1.89

Table 1: bulk density conditions of the soil samples.

2.1.2 Soil conditions

Table:reftab:bdtabel summarizes the moisture levels and densities of the soil samples used in DST, consisting of sandy soil with 12% clay, 6% silt, and 82% sand particles. The study examined three moisture levels - Dry, Moist, and Wet - and four bulk density levels, including Loose, Soft, Firm, and Compacted. There were 12 soil moisture and density combinations, and DST was performed for each combination with minimal variation within each level. The treatments were not replicated, as the data was primarily used for model development.

2.1.3 Test procedure

The shear box, a composite of upper and lower halves, is united through a locking pin, rendering it a singular unit. Following this, the base plate is affixed and positioned at the base, coupled with the non-porous grip plate placed above it. Given the dry nature of the soil under examination, selecting a non-porous grip plate is judicious. The shear box forms a square geometry, characterized by 6 x 6 x 3 cm dimensions. The vertical dimension (3 cm) is ascertained after placing the base and grip plates. To achieve the requisite density during the filling process, the mass of the soil is meticulously measured (mass of soil = density x volume of the box) and subsequently introduced into the shear box. Following soil filling, the friction plate is situated, followed by the placement of the load pad atop the friction plate. This comprehensive assembly is accommodated within a container affixed to the loading frame.

The loading frame orchestrates the application of vertical stress, where the magnitude of stress is established based on the stones located at the lever assembly's lower segment. Each stone administers a stress of **0**.**1**kg/cm^2. In alignment with the prescribed vertical stress (normal stress), the quantity of stones within the lever assembly is adjusted. The container housing the shear box is equipped with a proving ring, an instrumental component that measures the horizontal load *(Kg/cm^2)*. Correspondingly, a dial gauge is strategically situated to ascertain the shear box's associated displacement (mm).

The direct shear test is executed as a constant strain test, necessitating the application of a controlled strain rate of 1.25 mm/min. Subsequently, the locking pin is withdrawn, thereby decoupling the upper and lower sections of the shear box. The experiment's initiation involves the motor's activation, which imparts a horizontal load onto the shear box. With each progression of the dial gauge, the corresponding proving ring reading is meticulously noted. The reversal of the indicator's rotation within the proving ring marks the soil's failure point. The demonstrating proving ring underscores the horizontal load (shear stress), while the dial gauge reading concisely reflects the magnitude of displacement. This iterative process is recurrently undertaken across varying vertical loads, each introduced by adding an extra stone. The paired observations of corresponding proving ring and dial gauge readings are diligently recorded for each instance. The volume of the soil in the shear box was measured before test, and after test the soil sample was weighed, oven-dried at 105 C for 24 h, and weighed again to determine the soil moisture content and initial dry bulk density. The displacement (mm) was converted to strain percentage using thefollowing formula.

$$e(\%) = \frac{Di_f \quad Di_i}{H} * 100$$

(Di) initial and *(Df* final displacement values. H is the height of the specimen.

2.2 Model development and calibration

Here are some general assumptions that are often associated with the EDEM

1. **Particle Shape**: EDEM assumes particles are mostly round.
2. **Particle Rigidity**: Particles don't change shape, except when they hit each other.
3. **No Breaking**: EDEM doesn't automatically make particles break into smaller pieces.
4. **Bouncing and Sliding**: Particles can bounce and slide off each other.
5. **No Stickiness**: EDEM doesn't include stickiness between particles unless added.
6. **No Heat or Fluid Flow**: EDEM focuses on how particles move, not on heat or fluids.
7. **No Static Electricity**: EDEM doesn't account for electric charges on particles.

2.2.1 Model of direct shear test

To simulate the DSTs mentioned, a model was created using a shear box. The EDEM create geometry section was utilized to construct the box, which consisted of two square halves (upper and lower), a bottom base, and a top cover. The cross-section of the box was 60 X 60 mm, and each square was 25 mm tall, matching the dimensions used in laboratory tests. Soil particles in the direct shear box were represented by particles (balls) generated within the box (as seen in Fig.2a. The ball size was determined by a uniform distribution, ranging from 3 mm to 4 mm for the lower and upper values, respectively. The EDEM's three contact models *viz.,* Hertz-Mindlin contact (HM), the Hysteretic Spring (HS) model, and the Hertz-Mindlin with JKR (HM+JRK) was used to

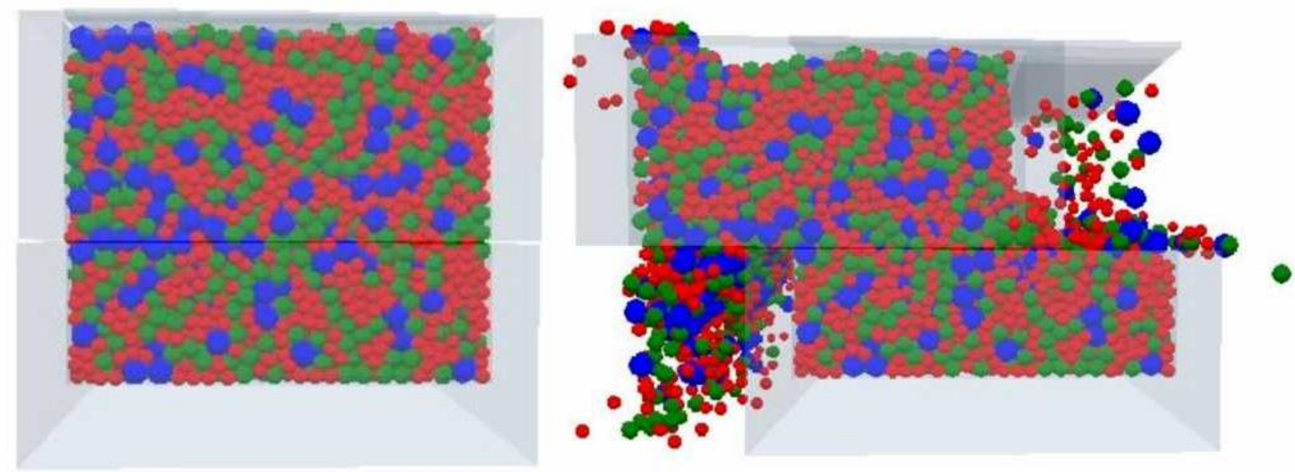

Figure 2: Virtual shear box with model particles: (a) before shearing; (b) after shearing describe the behavior of the contact between particles.

The Dry sandy soil alone model with two contact models (HM and HS). While moist and wet sand was modeled with two contact models (HS and HM+JRK). The details of the model used for simulating DST are tabulated in Tabel:2. The particle density of the model was initially set to match that of real soil, which is 2650 *kg/m*^{3}. However, achieving appropriate packing of the model particles was difficult due to their high porosity. To reach the bulk density range used in laboratory DSTs, a particle density of 1900 kg/m^3 was determined to be suitable through preliminary simulations. While the bulk density was varied as in the laboratory DSTs.

Model particles were generated and cycled to achieve equilibrium in the virtual shear box and ensure that the maximum contact force in the particle assembly was greater than the unbalanced force. To carry out virtual shear tests, a servo wall was used as the top wall of the shear box to apply a constant normal load, which was controlled by changing the wall velocity until it became equal to the desired normal load. Shearing was then conducted by keeping the top box stationary and horizontally displacing the bottom box at a desired speed, as shown in Fig.2b. The final step involved calibrating the micro-properties of the model particles to determine the sandy soil's properties.

Moisture level	**Density level**	**Contactmodel**
Dry	Loose	HM , HS
	Soft	HM , HS
	Firm	HM , HS
	Compact	HM , HS
Moist	Loose	HS , HM+JRK
	Soft	HS , HM+JRK
	Firm	HS , HM+JRK
	Compact	HS , HM+JRK
Wet	Loose	HS , HM+JRK
	Soft	HS , HM+JRK
	Firm	HS , HM+JRK
	Compact	HS , HM+JRK

Table 2: bulk density conditions of the soil samples.

2.2.2 Determination of the micro-properties of model particles

All models share six fundamental or base properties that are inherent to each of them. The six fundamental or base properties are Poisson's ratio(v), solid density(p), Young's modulus (E), coefficient of restitution (^R), coefficient of static friction ($p_{,s}$), and coefficient of rolling friction *(*$[i_r$). Not all base properties can be calibrated. Some of them need to be preselected before calibrations of others. The coefficient of rolling friction ($^\wedge_r$) represents the efficiency of energy conversion between kinetic and potential energy during the rolling motion of objects. For most solid-solid interfaces in everyday situations, *(*$[i_r$) is typically lower than the coefficient of static friction ($p_{,s}$). It is common for *(*$[i_r$) to be less than

1. The actual range of values can be quite broad, from near zero for very smooth or lubricated surfaces to higher values for rough or adhesive interfaces. In simulations of soil particles, higher *([ir)* values would result in particles being less likely to roll and more likely to remain in place or slide instead. The coefficient of rolling friction for soil is always less than 0.4. The *[i*$_r$ values used for simulation are 0.01, 0.1, and 0.3 for dry, moist, and wet soil, respectively.

The coefficient of restitution *([i*$_R$) is defined as the ratio of the relative velocity of separation to the relative velocity of approach after a collision. It represents how "bouncy" or "elastic" a collision is between two objects. It determines how kinetic energy is conserved or lost during the collision. $p,_R$ values can range from 0 to 1, with 0 indicating a perfectly inelastic collision (no rebound, all kinetic energy lost), and 1 indicating a perfectly elastic collision(complete rebound, no kinetic energy lost). The friction coefficient for sand soils is recommended to be between 0.30 and 0.50. The //$_R$ values used for simulation are 0.5, 0.45, and 0.4 for dry, moist, and wet soil, respectively.

Using DST results, Young's modulus(E) was determined by plotting stressvs. strain. The slope of the linear portion of the plot provides the modulus. The tangent of the slope of the normal vs. shear stress plot gives the frictional angle (^>). The Poisson's ratio(v) is determined by following the formula

1 — *sin6*

v = -- '■—*7*

1 + sin0

The angle of repose test is conducted in laboratory. coefficient of static friction (^$_s$) is determined by following formula-1 h *[i*$_s$ = *tan* — *r* h is The height and d is the diameter pile of soil.

The //$_s$ is determined from the angle of the repose test. The value of s varies depending on the specific properties of the soil and contacting surfaces, with recommendations for sand soils ranging between 0.30 and 0.50.

The The Hertz-Mindlin is the default model used in EDEM due to its accurate and efficient force calculation. This model's normal force component is based on Hertzian contact theory (Hertz 1882). The tangential force model is based on Mindlin-Deresiewicz's work (Mindlin 1949) (Mindlin and Deresiewicz1953). This model has no micro-properties except the base parameter. Hertz-Mindlin with JKR (Johnson-Kendall-Roberts) Cohesion is a cohesion contact model that accounts for the influence of Van der Waals forces within the contact zone and allows the user to model strongly adhesive systems. Surface energy is a micro-properties of this model, which is material's ability to retain moisture/charge on its surface. The amount of surface energy influences the adhesion of the material. The SI unit of surface energy is J/ms. The surface energy value was adjusted in the simulation process; preliminary simulations in this study showed no noticeable changes in resultant soil shear properties when changing the for dry soil. The there is significant change is observed when moisture is added. The surface energy for three soil states, dry, moist, and wet, is 0.2J/m2, 0.1 J/m2, and 0 J/m2, respectively is used in the study.

The Hysteretic Spring contact model includes plastic deformation behaviors in the contact mechanics equations, resulting in particles behaving elastically up to predefined stress. Once this stress is exceeded, the particles undergo plastic deformation. The damping factor and stiffness factor is important micro-properties in this mode. The damping factor is this dimensionless parameter that controls the amount of velocity-dependent damping. Stiffness factor: This dimensionless parameter is defined as the ratio of tangential stiffness (K_t) to normal (K_n)loading stiffness and is used in the calculation of tangential forces at the contact. According to the literature, the typical value of this parameter is in the range between 0.7 and 1. In this study the particle normal and tangential stiffness were set as same, meaning that K_t/K_n = 1. The particle stiffness (K_n) is calibrated with the measured yield forces.

3. Results And Discussion

3.1 Laboratory test results

3.1.1 Soil yield forces

For model calibration purposes, DSTs were used to examine yield forces. Yield points were taken from all force-displacement curves of the 12 treatment combinations, and were plotted with soil moisture levels (Fig.3). The Compact soil had the highest yield forces across all soil moisture levels, followed by the Firm soil. This held true for all three normal loads. The Soft and Loose soils had lower yield forces. The data was re-plotted to demonstrate the effects of soil moisture level on yield forces (Fig.4). Under all normal loads, the Dry soil had higher yield forces than the Moist and Wet soils across all soil bulk density levels.

To summarize, the differences in yield force between the Loose and Soft soils were consistent across the three normal loads, and sometimes had similar yield forces (Fig.3), (Fig.4). Based on these results, yield forces of the Loose and Soft soils were combined in model calibrations. As a result, calibration was only required for six combinations instead of the original 12 combinations of soil moisture and density levels.

Figure 3: Comparisons of yield forces between the soil bulk density levels under different moisture levels and normal loads *(F_n)*

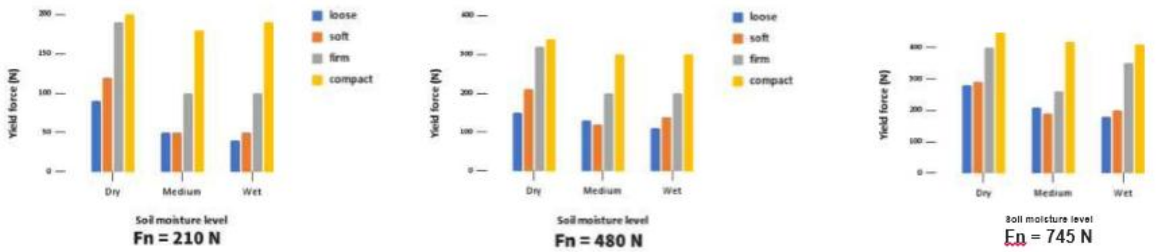

- loose
- soft
- firm
- compj

Figure 4: Comparisons of yield forces between the soil moisture levels under different bulk density levels and normal loads *(F_n)*

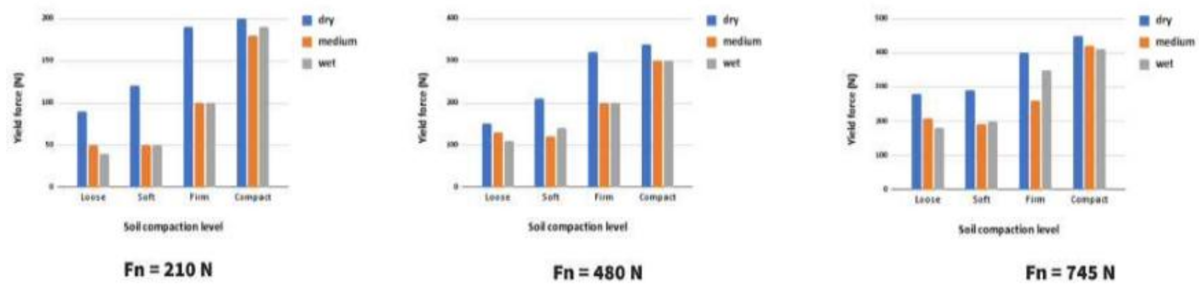

The parameters for the model were determined using the soil internal friction angle (0) and cohesion (c) from DST. This data was obtained from yield force data, which was then converted to yield stresses based on the given area of the shear surface of the shear box. The normal loads in force were also converted to stresses based on the given cross-sectional area of the soil sample in the shear box. A linear trend line was created from the yield and normal stresses, with 0 being determined as the slope of the trend line, and c being determined as the intersection. The trends of treatment effects on 0 and c values were similar to those of yield forces, and as such, they are presented for six soil moisture and density combinations in Table 2.

Property	**Average**		Dry		Moist				wet	
	19.5	18	23	25	14.5	19.5	25	11.5	17	22
c	11303	10648	24975	34463	1192	4680	12856	1013	3931	7970

Table 3: Soil internal friction angle and cohesion obtained from laboratory direct shear tests.

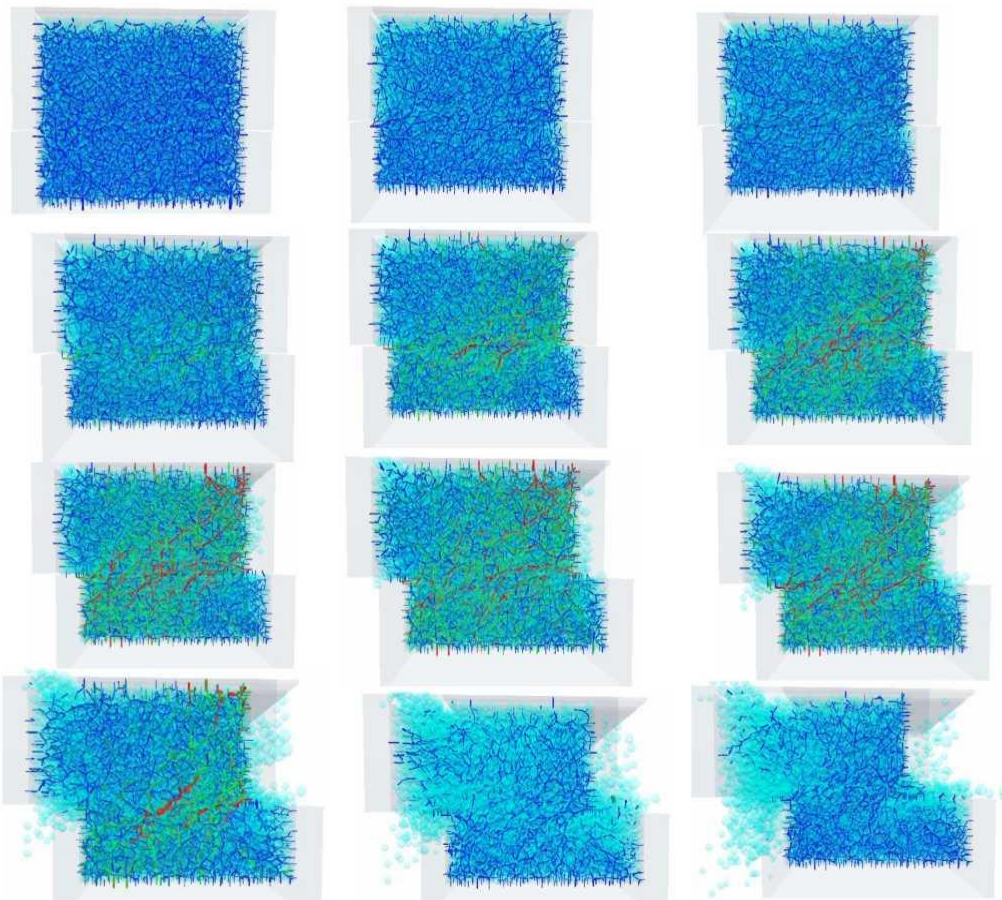

Figure 5: Particle instantaneous velocity field from simulations

3.2 Simulation and calibration results

3.2.1 Model behaviors

Initial virtual direct shear tests were conducted to test the model's soil shear behavior simulation. A picture of the velocity field near the end of a virtual direct shear test is shown in Figure5, which displays the particle instantaneous velocity field.

During the virtual test, most particles in the bottom box flowed horizontally in the direction of the shear force. The balls in the upper right corner of the top box had zero vLoose 1.45 Soft 1.60 Firm 1.75 Compact 1.90elocities because the top ring remained stationary throughout the test. Towards the end of shearing, particles in the lower left corner of the top ring flowed downwards due to theoffset of the top box concerning the bottom ring. These observations align with Liu et al.'s DEM simulation of a granular material's direct shear test. All virtual direct shear tests were conducted using the same normal loads and shear speed as those in the laboratory DSTs.

$$RE = \frac{\mathbf{100}}{n} \quad \underline{S\text{-}M}$$

Two models simulated the soil in dry, moist, and wet conditions. The simulated values were then used to conduct a virtual shear test for three normal loads (210, 480, and 745 N), generating three shear force vs. strain curves. Upon comparison with the measured curve (Fig.6), it was observed that the simulated curve had a similar trend as the measured

as

one, but varied depending on the model used. The simulated curves often showed more apparent yield points. To further illustrate this, Fig.6a, Fig.6b, and Fig.6c show the comparative curves of the measured and two simulated models. The yield forces for both the simulated and measured curves are tabulated in Tabel4. Their agreement was evaluated using the relative error (RE), which was defined where RE = relative error (%), n = number of observations (n = 3 in this case), S = simulated yield force (N), M = measured yield force (N)

The HM model was more effective for sandy soil in dry conditions based on the results. The HS model performed better in moist conditions, while the HM+JKR model was the most effective in wet conditions. Therefore, the HM model had the lowest RE (1.41%) for dry soil, the HS model(1.00%) was similar for moist soil, and the HM+JKR model(0.33%) was the most effective for wet soil.

Using the calibrated model parameters allows for the simulation of various soil behaviors, including particle contact force velocity fields, vertical displacement, and strain energy at the particle level. Additionally, these parameters can be utilized in simulations involving soil-engaging tools, such as tillage tools, seed openers, and fertilizer application tools, with the soil.

Moisture	**Model**	**Normal Force (N)**	**Simulated yield Force (N)**	**Measured yield force (N)**	**Relative error, RE (%)**
Dry	HM	210	220	200	3.33
	HM	480	355	340	1.47
	HM	745	490	470	**1.41**
	HS	210	170	200	4.99
	HS	480	250	340	8.82
	HS	745	280	470	13.47
Moist	HS	210	170	180	1.85
	HS	480	285	300	1.66
	HS	745	443	430	**1.00**
	HM+JKR	210	115	180	12.03
	HM+JKR	480	205	300	10.55
	HM+JKR	745	230	430	15.50
Wet	HS	210	160	190	5.26
	HS	480	240	300	6.66
	HS	745	270	400	10.83
	HM+JKR	210	180	190	1.75
	HM+JKR	480	289	300	1.22
	HM+JKR	745	396	400	**0.33**

Table 4: Calibration process using the Dry Compact soil condition

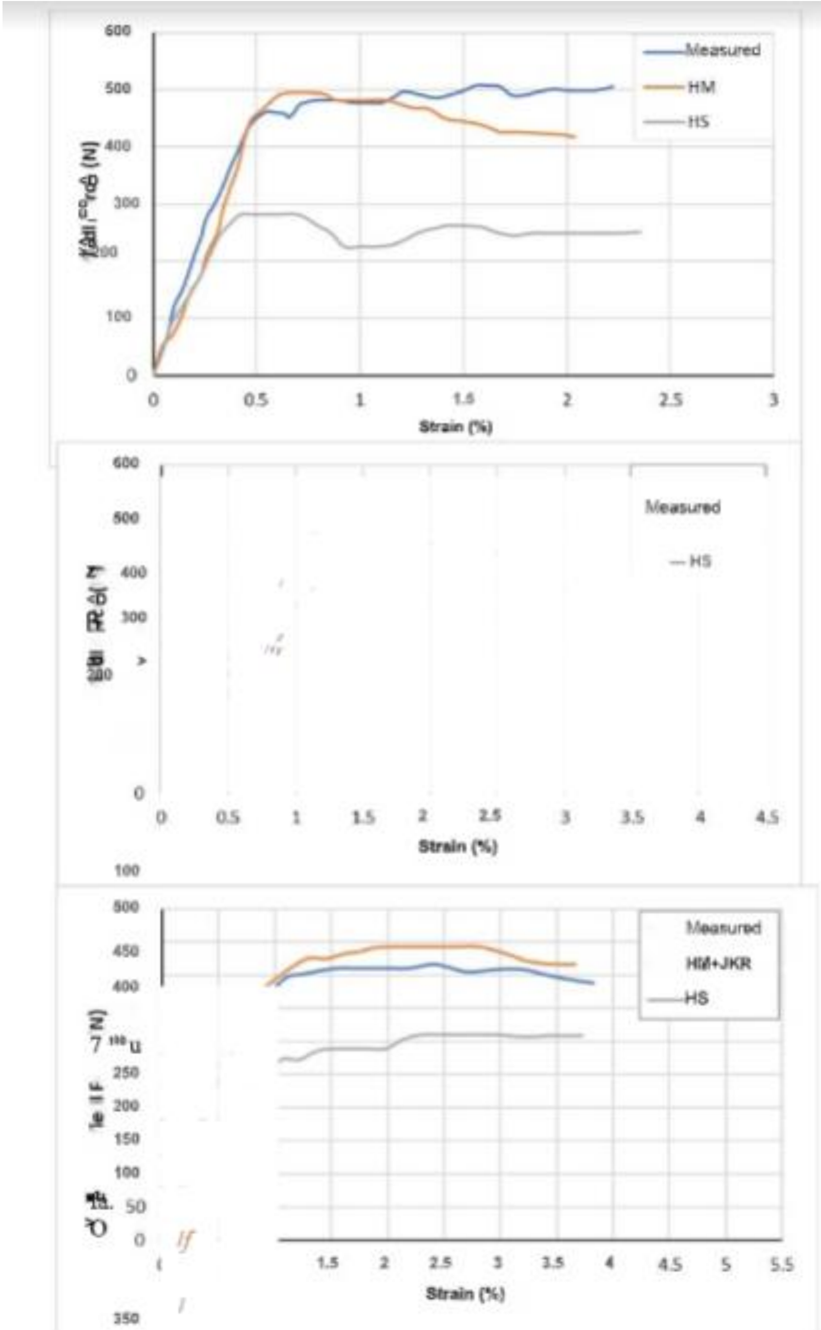

Figure 6: Typical shear force displacement (horizontal) curve from the laboratory DST and simulated DST for the Compacted dry (a) , moist(b) and wet(c) soils

4. Conclusion

The research paper has been carefully examined, and the results have been thoroughly analyzed. The behavior of sandy soil has been successfully simulated and calibrated using the Discrete Element Method (DEM) in various moisture and density conditions. The performance of three different contact models, namely Hertz-Mindlin (HM), Hysteretic Spring (HS), and Hertz-Mindlin with JKR (HM+JKR), has been assessed to replicate the intricate interactions and mechanical responses exhibited by sandy soil particles under varying loading conditions. The simulation results were compared with laboratory Direct Shear Tests (DSTs) for validation. It was found that the HM model performed effectively for dry soil conditions, the HS model for moist soil, and the HM+JKR model for wet soil. The relative errors between the simulated and measured yield forces were within acceptable limits for all three models, confirming their effectiveness in representing soil behavior. These calibrated models will be valuable in future simulations and analyses of soil-tool interactions in agriculture and geotechnical engineering applications. The research has contributed to a better understanding of the Discrete Element Method's capabilities in modeling soil mechanics and provided insights into selecting appropriate contact models for different soil conditions.

5. References

[1] Coetzee, C. and Els, D. (2009). Calibration of discrete element parameters and the modelling of silo discharge and bucket filling. *Computers and electronics in agriculture,* 65(2):198-212.

[2] Cundall, P. A. and Strack, O. D. (1979). A discrete numerical model for granular assemblies. *geotechnique,* 29(1):47-65.

[3] Gitau, A., Gumbe, L., and Mwea, S. (2008). Mechanical behavior of a hard-setting luvisol soil as influenced by soil water and effective confining stress. *Agricultural Engineering International: CIGR Journal.*

[4] Kadau, D., Schwesig, D., Theuerkauf, J., and Wolf, D. E. (2006). Influence of particle elasticity in shear testers. *Granular Matter,* 8:35-40.

[5] Kezdi, A. (1979). Soil physics-selected topics-developments in geotechnical engineering-25. Technical report.

[6] Khot, L. R., Salokhe, V. M., Jayasuriya, H., and Nakashima, H. (2007). Experimental validation of distinct element simulation for dynamic wheel-soil interaction. *Journal of Terramechanics,* 44(6):429-437.

[7] Li, H., Li, Y., Tang, Z., Xu, L., and Zhao, Z. (2011). Numerical simulation and analysis of vibration screening based on edem. *Transactions of the Chinese Society of Agricultural Engineering,* 27(5):117-121.

[8] Li, J., Tong, J., Hu, B., Wang, H., Mao, C., and Ma, Y. (2019). Calibration of parameters of interaction between clayey black soil with different moisture content and soil-engaging component in northeast china. *Transactions of the CSAE,* 35(6):130-140.

[9] McKyes, E. (1985). *Soil cutting and tillage.* Elsevier.

[10] Nitka, M. and Grabowski, A. (2021). Shear band evolution phenomena in direct shear test modelled with dem. *Powder Technology,* 391:369-384.

[11] Potyondy, D. O. and Cundall, P. (2004). A bonded-particle model for rock. *International journal of rock mechanics and mining sciences,* 41(8):1329-1364.

[12] Shi, Y., Rex, S. X., Wang, X., Hu, Z., Newman, D., and Ding, W. (2019). Numerical simulation and field tests of minimum-tillage planter with straw smashing and strip laying based on edem software. *Computers and Electronics in Agriculture,* 166:105021.

[13] Thornton, C. and Zhang, L. (2003). Numerical simulations of the direct shear test. *Chemical Engineering & Technology: Industrial Chemistry-Plant Equipment-Process Engineering-Biotechnology,* 26(2):153-156.

[14] Van der Linde, J. (2007). *Discrete element modeling of a vibratory subsoiler.* PhD thesis, Stellenbosch: University of Stellenbosch.

[15] Zhang, Q., Li, B., Xu, Y., Zhang, J., Li, M., and Tong, J. (2021). Effects of biomimetic press roller type, material, velocity and packing force on compaction characteristics. *Transactions of the ASABE.*

[16] Zhang, R. and Li, J. (2006). Simulation on mechanical behavior of cohesive soil by distinct element method. *Journal of Terramechanics,* 43(3):303-316.